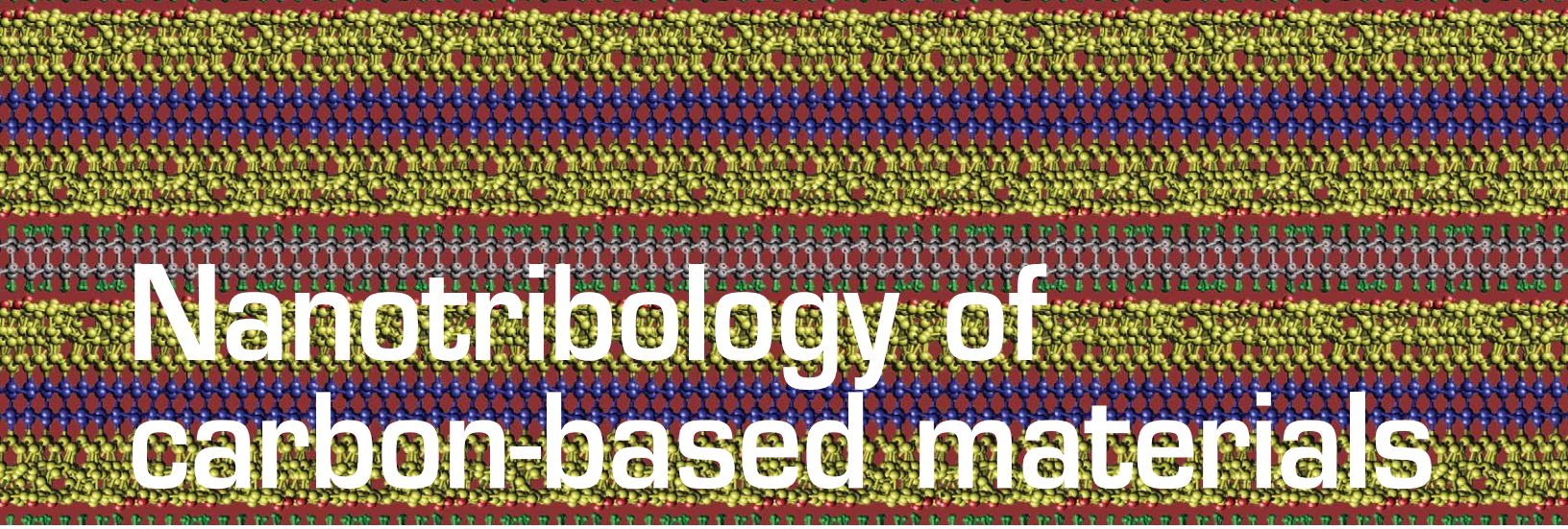

Nanotribology of carbon-based materials

The dominance of surface effects at the nanoscale implies that nanotechnology applications involving contacting, moving components can be critically limited by the tribological behavior of the interacting materials. Carbon-based materials have tremendous potential here because of their robust and often unsurpassed tribological performance. We review some recent insights gained by nanotribology studies of various forms of carbon, with an emphasis on thin film materials.

David S. Grierson[1] and Robert W. Carpick[2]*

[1] *Engineering Physics Department, University of Wisconsin-Madison, Madison, WI, 53706, USA*

[2] *Department of Mechanical Engineering and Applied Mechanics, University of Pennsylvania, Philadelphia, PA, 19104, USA*

**E-mail: carpick@seas.upenn.edu*

Carbon-based systems comprise an impressively broad and continually expanding range of materials, from the building blocks of biology to carbon allotropes with extreme and exotic properties such as nanotubes, buckyballs, graphene[1], and diamondoids[2]. The myriad of stable forms that carbon can adopt is largely because of its ability to hybridize in multiple stable bonding states, and to bond strongly with many other atoms, including hydrogen.

Many carbon-based thin films have been developed to address a broad range of coating applications, including uses that demand outstanding tribological performance in a wide variety of operating environments. The most critical compositional variables are the distribution of the carbon hybridization states (specifically, sp^2 versus sp^3 bonds) and the atomic H content. This compositional phase space is illustrated in Fig. 1[3,4]. Dopants such as Si, F, N, B, and O can be used to modify surface energy, mechanical properties, and electrical conductivity.

Here we particularly focus on: (i) ordered, highly sp^3-bonded materials (i.e. diamond in single crystal or polycrystalline form); (ii) amorphous, highly sp^3-bonded materials, often referred to as tetrahedral amorphous carbon (ta-C); (iii) amorphous films with a mixture of sp^2 and sp^3 bonding, necessarily stabilized with H, often generically known as diamond-like carbon (DLC); and (iv) ordered, sp^2-bonded carbon (i.e. graphite).

At the macroscopic scale, the mechanical and tribological properties of these materials are nothing short of astonishing. Diamond, the stiffest and hardest material known, can be grown in nanocrystalline thin-film form with nearly equivalent mechanical performance[5,6]. Friction coefficients are below 0.05, which is as slippery as common ice, and wear rates correspond to mere fractions of an atomic layer per pass of the sliding interface, with no lubricant needed[7]. DLC films, grown in a particular form known as near-frictionless carbon (NFC), can exhibit friction coefficients as low as 0.001 and wear rates even lower than diamond[8].

Successful tribological applications of diamond films include coatings for tools, optical components, biological implants, and more recently, as structural materials for microelectromechanical systems

ISSN:1748 0132 © Elsevier Ltd 2007

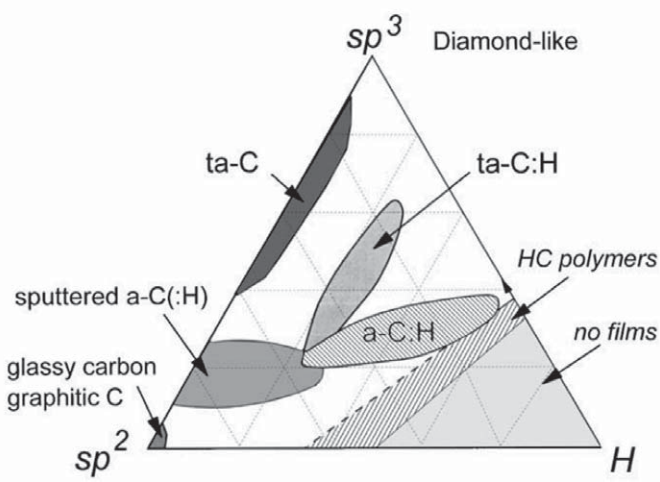

Fig. 1 Robertson diagram illustrating the different compositions of common carbon-based materials. (Adapted with permission from[4]. © 2002 Elsevier.)

(MEMS) resonators and other related devices[9–11]. Applications for DLC films are significantly more established, with uses as hard disk coatings, aerospace bearings, automotive parts, orthopedic implants, and cutting blades[8].

However, the widespread use of carbon films at all scales has been hampered by several issues including film stress, film adhesion, growth rates, and uniformity. More fundamentally, carbon films can be highly sensitive to the environment. For example, the tribological performance of DLC degrades significantly when water is present[12–16]. In contrast, diamond films can exhibit extremely poor performance in vacuum or dry conditions[17–20], with friction coefficients exceeding 1.0, and wear becoming severe. The effects of local atomic order, orientation, and chemistry at interfaces become important for nanoscale applications as well, but these factors are not yet understood.

The notable failure to commercialize any Si-based MEMS devices that have sliding parts in contact[21] highlights the need for alternative materials for micro- and nanoscale devices and systems. Carbon-based materials may be the key. Here we discuss the science of carbon nanotribology to highlight the current understanding and remaining challenges for evaluating the potential of carbon-based materials for nanosystems.

Single asperity friction

Studying the physical origins of tribology requires examining well-defined interfaces. Thus, experiments and models often focus on single asperity contacts (i.e. where there is a single, continuous contact area). This avoids significant complexities brought about by surface roughness.

The atomic force microscope (AFM) is the most widely used tool for nanoscale single asperity studies (Fig. 2), and molecular dynamics (MD) has been used extensively to simulate nanotribological interfaces. MD is extremely powerful, since all forces, displacements, and velocities are resolved atomistically, allowing stresses, strains, temperatures, and vibrations to be determined. Some potentials also allow chemical reactions and material transformations to be studied. The information can be examined both to reveal and quantify the physical mechanisms occurring at a buried interface. Currently, only classical, not quantum, MD must be used to have any hope of reaching a simulation size (i.e. number of atoms) comparable to state-of-the-art AFM experiments, and so the empirically derived classical potentials may be inaccurate. In addition, the time scales of the simulations are extremely short (10^{-15} s time steps; ~10^{-9} s simulation times).

Key challenges with AFM include the calibration of normal and lateral forces, control of the tip surface composition, and preservation of the tip geometry during experimental testing. Previous AFM-based work concluded that friction in many solid-solid nanocontacts below the wear threshold is proportional to the true contact area (i.e. number of interfacial atoms)[22–28]. In other words, the friction force F_f for a single asperity contact is given by:

$$F_f = \tau A \quad (1)$$

where A is the interfacial contact area and τ is the interfacial shear strength. Thus, τ represents the frictional force per interfacial atom. The contact area A typically does not vary linearly with load; for example, in the classical theory of Hertz[29], the contact area is proportional to the load raised to the 2/3 power ($L^{2/3}$). These observations are in stark contrast to the macroscopic observation of a friction coefficient (i.e. that friction is linearly proportional to applied load).

The shear strength may be a constant, or it may have a dependence on the contact pressure or applied shear[30]. A linear dependence on contact pressure combined with eq 1 results in a linear term connecting friction and load, thus matching the familiar macroscopic result but now with more physical insight. What remains unresolved is how the interatomic forces determine the value of τ itself.

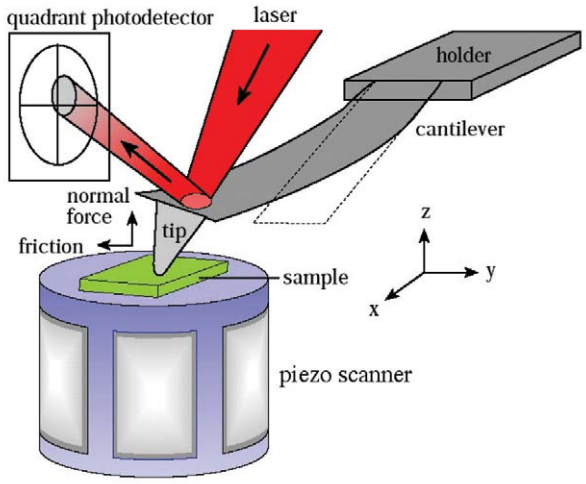

Fig. 2 Schematic of a typical AFM instrument. A nanoscale single asperity contact is formed between the tip and the sample's surface. Normal and lateral forces and displacements are measured with atomic-scale resolution. The environmental conditions can be controlled over a wide range.

One can also measure the interfacial work of adhesion (adhesion energy per interfacial atom), given by $\gamma = \gamma_1 + \gamma_2 - \gamma_{12}$, where γ_1 and γ_2 are the tip and sample surface energies, respectively, and γ_{12} is the interfacial energy[31]. All interfacial forces are encompassed by γ, which represents the work per unit area required to separate the surfaces from contact to infinity. If the tip is 'round', i.e. paraboloidal, and makes contact with a flat elastic surface, the behavior spans a spectrum from the Johnson-Kendall-Roberts (JKR) model[32] (for large tips and compliant materials with strong, short-range adhesion) to the Derjaguin-Müller-Toporov (DMT) model[33] (for small tips and stiff materials with weak, long-range adhesion). In an AFM experiment, γ is determined from the force F_{PO} required to pull a tip of radius R out of contact with the surface:

$$\gamma = \frac{-F_{PO}}{\chi \pi R} \qquad (2)$$

where χ ranges monotonically from 1.5 (JKR) to 2 (DMT). In many studies, continuum mechanics appears to provide an accurate description of the nanometer-scale contact area A and other contact properties[22]. Key assumptions to bear in mind are homogeneity, isotropy, linearity, and elasticity of the materials; several modified continuum contact mechanical models describing other cases have been derived[34,35]. However, more fundamentally, Luan and Robbins[36,37] have recently explored nanoscale contacts using atomistic simulations, and found cases where continuum mechanics breaks down altogether. This presents a challenge for properly analyzing the contact properties in this atomistic limit.

The process of wear, which is of great importance for applications, is more difficult to quantify in terms of fundamental physical parameters. So far, quantification of the loads and stresses that initiate wear, and characterization of changes in asperity shape, represent the extent to which AFM experiments have progressed; MD simulations that model bond breaking and atomic rearrangement are able to provide valuable insight into the nature of this process.

Influence of applied load

Several single asperity AFM studies of carbon-based materials have been performed. While the samples used are all carbon-based, the same is not always true for the tips. Commercial AFM tips are typically composed of Si or Si_3N_4, with only a few other tip coatings available. Researchers have taken up the challenge of coating the tip itself in only a few studies so far (this is discussed further in the section on carbon nanotips). Coating the tip with the same material as the sample has the critical advantage of matching the interface that would be found in an actual device composed entirely of that material.

Several studies have found that the DMT model accurately describes the variation of friction with load[27,38–41]. That is, eq 1 is assumed to be valid, the DMT equation for contact area is fitted to the friction data, and a shear strength value is then extracted. Examples are shown in Figs. 3a and 3b. This DMT-like behavior is expected for these materials since the model applies to interfaces involving small tip radii, low adhesion, and high elastic moduli. A more recent study of single-crystal diamond has found behavior closer to the JKR regime, which contradicts expectations[42]. Significant variation from one location to the next on the sample has been observed, suggesting a strong sensitivity to defects (Fig. 3c). Further modeling and experimental work is required to clarify the exact role that contact area plays at the nanoscale.

In cases where friction-load relationships have been measured on a variety of different carbon-based materials in the same study, it has consistently been found that highly oriented pyrolytic graphite (HOPG) is the least resistant to sliding (Fig. 3b), followed by diamond, and then DLC[28,38,39]. However, the tribological characteristics of any interface can be highly dependent on orientation, topography,

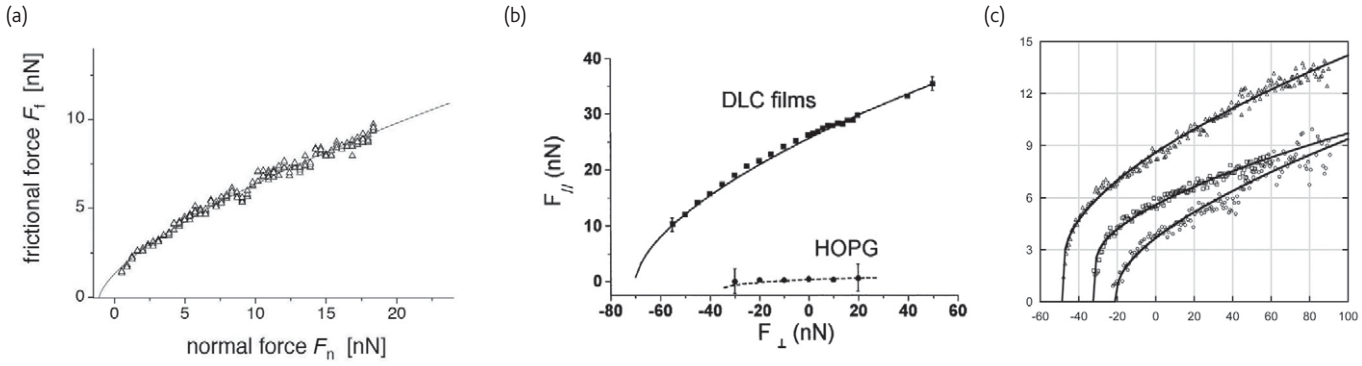

Fig. 3 (a) Friction versus load for a hydrocarbon tip on a DLC surface, and a fit of the DMT model. (b) Load-dependent measurements with a hydrocarbon tip representing the mean frictional response of DLC films (squares) and HOPG samples (circles). Experimental data are fitted with the DMT model. (c) Three averages of different friction versus load data sets depicting the type of variation in friction force observed for different locations on a given grain. This particular example is for the 45 nm hydrocarbon-coated tip scanning in the [112] direction on a (111)-oriented grain. The curve-fits are fits to a model for contact area that is intermediate to the JKR and DMT limits. (Part (a) reproduced with permission from[39]. © 1997 American Physical Society. Part (b) reproduced with permission from[38]. © 2003 Elsevier. Part (c) reproduced with permission from[42]. © 2007 American Chemical Society.)

chemical composition, bonding structure, elastic/plastic properties, and environment. Careful measurements of these factors must be considered if the physical origins of friction and energy dissipation are to be determined.

Influence of orientation

Diamond

At the macroscopic scale, diamond single crystals show strong orientation effects, where friction and wear depend on both the surface orientation and the sliding direction[43]. The findings at the nanoscale are considerably different. In part, this is because of the avoidance of wear, but it may also be as a result of an enhanced influence of local atomic interactions.

In 1993, a team at IBM studied single-crystal, H-terminated diamond (111) and (001) surfaces with a 30 nm radius diamond AFM tip[44]. Average friction force values were obtained over several

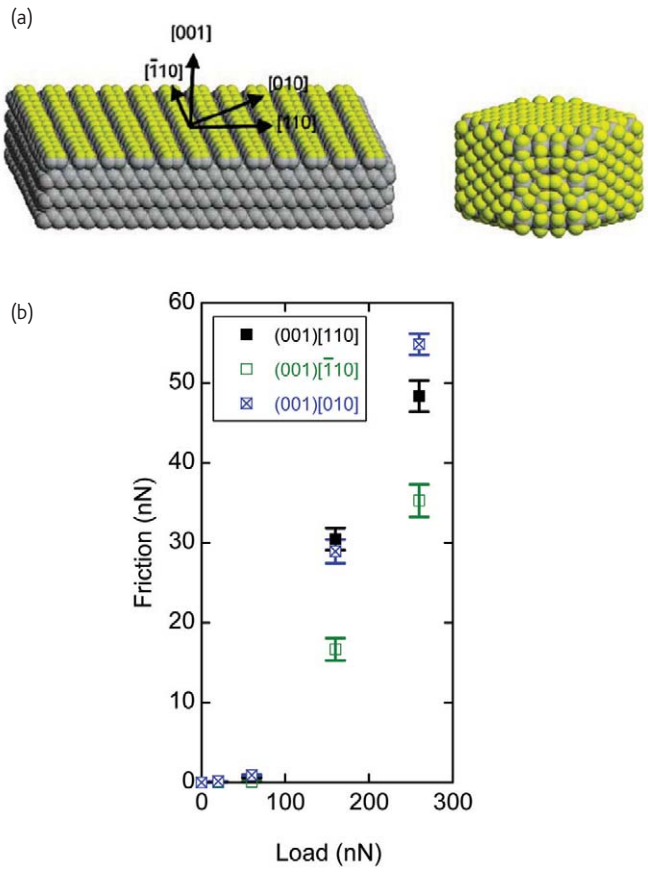

Fig. 4(a) The H-terminated diamond surface used in the MD simulations[42] showing the 2 x 1 reconstruction and one of the tips used (in this case, a flat nanowire tip). (b) Average friction versus load data, from the MD simulations[42], at 300 K using the diamond nanowire tip shown in (a). Diamond surface and sliding directions are given in the legend. All results are similar, except for the reduced friction seen when sliding along the [$\bar{1}$10] direction on the (001) surface. (Reproduced with permission from[42]. © 2007 American Chemical Society.)

experiments and no difference was observed between the two surfaces except for qualitative differences in the friction images, attributable to the different lattice spacings and orientations. Atomic-scale variations in friction were seen; this 'stick-slip' effect is described further in the next section.

Further studies of orientation effects have exposed more quantitative differences between H-terminated diamond surfaces[42,45]. In a combined MD and AFM study, again no dependence of shear strength on surface orientation or sliding direction was found, except in one case: sliding on the (001) surface with a (2 x 1) reconstruction[42]. Both MD and AFM found reduced friction when sliding on this surface compared with all others, which was attributed to the anisotropic dimer rows (Fig. 4) produced by the (2 x 1) reconstruction, showing that the local orientation of atomic bonds indeed affects nanoscale friction. Further work is needed, as the MD and AFM experiments used different tips and scanning velocities, and the MD simulations did not include adhesive interactions. The (111) surfaces exhibited lower adhesion compared with (001) experimentally, an observation that has not yet been explained theoretically, but which has significant consequences for applications where adhesion is undesirable.

Graphite and the effect of superlubricity

When an AFM tip is sheared over the surface of a crystal lattice, it often moves in an unstable 'stick-slip' pattern that matches the lattice. This was first observed on graphite[46] and has since been reported on many other materials including diamond[20,44]. Essentially, it occurs because the compliance of the system (cantilever, tip, and contact zone) stores energy as shear is applied. This energy is suddenly released when the lateral force gradient in the sliding direction drops below the net system stiffness, the essence of mechanical instability. Since the lateral interaction force is necessarily periodic by virtue of the symmetry of the crystal surface, the stick-slip behavior repeats once every lattice site, creating stunning images that match the lattice periodicity. An example from a graphite surface is shown in Fig 5a. Stick-slip behavior leads to an unnecessary buildup and dissipation of energy. It has been shown that the effect gets more severe at higher loads, and transitions to doubled periodicity have been observed on graphite[47], in qualitative agreement with theoretical predictions[47,48].

Recently, researchers have suppressed the stick-slip instability[47,49,50]. The remaining frictional dissipation is below recordable values and the phenomenon has been labeled (perhaps misleadingly) 'superlubricity'. Regardless, friction is dramatically lower.

One way to achieve this transition to instability-free low friction is to obliterate the periodicity of the lateral potential by making the interface incommensurate. This was realized experimentally for graphite by using a graphite flake fortuitously attached to the tip of an advanced AFM allowing three-dimensional force measurement[51]. Rotating the sample with respect to the tip brings the interface

(a)

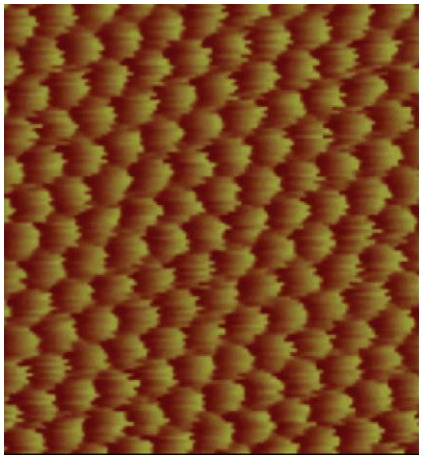

(b)

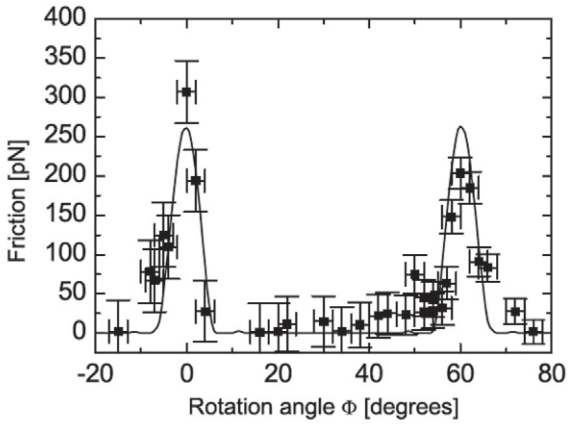

Fig. 5 (a) 2.5 nm x 2.5 nm lateral force image of a HOPG sample showing atomic lattice stick-slip behavior with a periodicity of ~0.25 nm, which corresponds to the HOPG lattice spacing of 0.246 nm. Experimental details are given in[47]. (b) Average force of friction force plotted versus the angle of rotation of the graphite sample. Two sharp peaks are observed at 0° and 61°, respectively, with ultralow friction in between. The solid curve shows results from a model calculation. (Part (b) reproduced with permission from[51]. © 2004 American Physical Society.)

into commensurability only at prescribed orientations (Fig. 5b). The incommensurability results in reduced friction by orders of magnitude compared with commensurate sliding[52]. This discovery provides a possible explanation for the exceptional lubricity of macroscale graphite solid lubricants, and suggests incommensurability as a design rule for achieving low friction. This may also account for the observation of low friction in the sliding of nested carbon nanotubes[53].

Influence of film composition

The chemical composition of a film, particularly at its surface, also influences nanoscale friction and wear. A predictive understanding of this relationship is yet to be found, but we review results and comment on the emerging trends here.

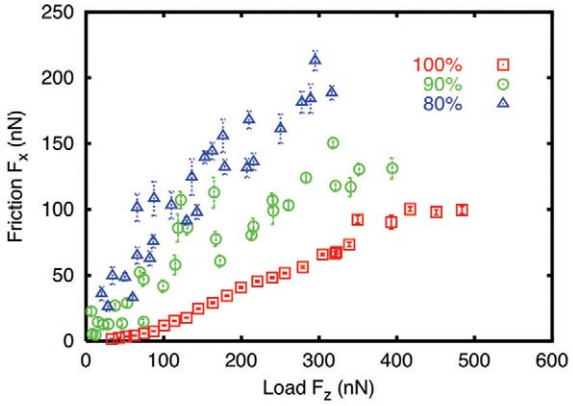

Fig. 6 Friction curves for the thin-film system with a counterface that is fully or 100% H-terminated (open squares), 90% H-terminated (filled squares), and 80% H-terminated (open circles). (Reproduced with permission from[56]. © 2002 American Chemical Society.)

Surface chemistry

The low macroscopic friction of diamond in air (μ = 0.05–0.1) has been attributed to the passivation of the surface by –H and –OH groups[19,54] and/or by the production of lubricious sp^2-bonded species[7,55]. Nanotribology studies put these ideas to the test, and a significant recent success has been the clear demonstration that –H termination reduces nanoscale friction dramatically.

The frictional properties of a diamond (111) single crystal surface have been studied using a Si AFM tip in ultrahigh vacuum (UHV), and the presence or absence of surface H was monitored by low-energy electron diffraction (LEED)[20]. Removal of the H from the surface causes an increase in the average friction coefficient by more than two orders of magnitude compared with the H-terminated surface for loads up to 30 nN. This is a clear, convincing example of how dangling bonds can bridge an interface and increase the contribution of adhesion to friction, and how passivation of those reactive bonds can reduce those forces in a dramatic way.

Complementary MD simulations have been conducted to investigate this passivation effect of H on diamond (111) surfaces by terminating the diamond with 80%, 90%, and 100% saturation[56]. An amorphous, H-free carbon probe is slid with variable load, and the resultant friction forces are calculated. Decreasing the saturation level of the diamond surface increases the friction, in qualitative agreement with the experimental study (Fig. 6). It has also been observed that a lower fractional coverage of H allows for tribochemical reactions to occur at lower loads than the 100% terminated case, thus increasing adhesion and wear. An MD study by Zhang *et al.*[57] compares friction coefficients between two DLC-like surfaces in sliding contact before and after 100% hydrogenation, and finds that surface hydrogenation reduces the friction coefficient there as well.

To model and visualize the dissociation and subsequent adsorption of H_2 gas and H_2O molecules on diamond, Qi *et al.*[58] have implemented density functional theory (DFT) calculations of

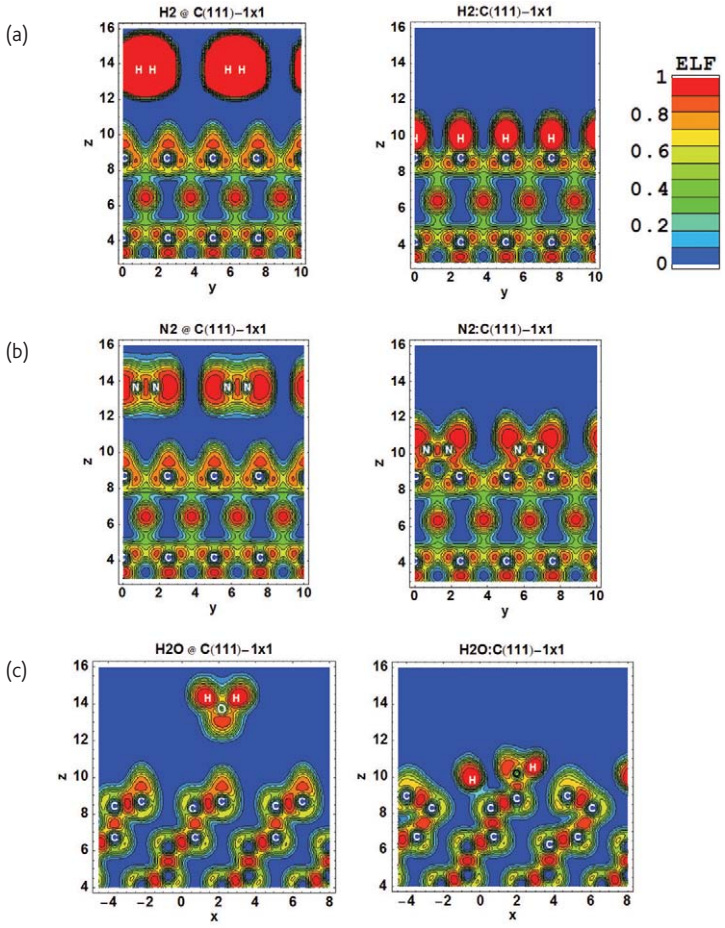

Fig. 7 Electron localization function (ELF) contour plots for the unadsorbed (left side) and adsorbed (right side) states of (a) H_2, (b) N_2, and (c) H_2O molecules interacting with diamond (111) surfaces. ELF = 1 corresponds to localization (i.e., a covalent bond), and ELF = 0.5 corresponds to electron-gas-like pair probability (i.e., a metallic bond). The ELF is undefined for values less than 0.5. (Reproduced with permission from[58]. © 2006 Elsevier.)

diamond (111) surfaces interacting with environmental species. They have employed the electron localization function (ELF) to generate contour plots of electron localization versus position (Fig. 7). These calculations suggest that adsorption and dissociation of H_2 at the surface is highly favored and results in strong covalent C–H bonding. Water dissociates into OH and H where OH then forms a covalent bond with carbon and H sits at a bridge site between two carbon atoms. Furthermore, the work of adhesion has been calculated to be low for both H-terminated and OH-terminated interfaces, respectively. H-terminated (111) surfaces required 8 mJm^{-2} for separation, and the OH-terminated (111) surfaces required 20 mJm^{-2} for separation.

The surface chemistry and nanotribology of the underside of ultrananocrystalline diamond (UNCD) films have been investigated with tungsten carbide[59] and diamond[60] AFM tips in ambient air to determine the effect of H-termination. Fully hydrogenating the surface removes sp^2-bonded carbon and oxygen, and correspondingly a reduction of both adhesion and friction results (Fig. 8). Thus, the passivating effect of H on nanocrystalline diamond in air has been

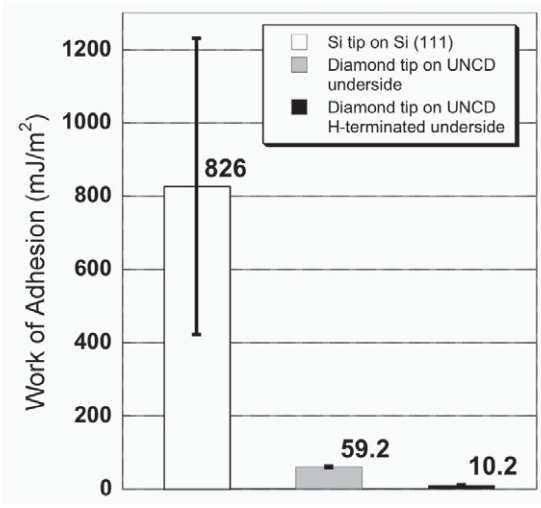

Fig. 8 Work of adhesion between a diamond tip and UNCD surfaces before and after H-termination. Results for a Si tip making contact with a single crystal Si (111) wafer after cleaning in piranha solution is included for comparison. (Reproduced with permission from[60]. © 2007 American Physical Society.)

demonstrated. In fact, the work of adhesion measured between the diamond tip and the hydrogenated UNCD surface is 10.4 ± 4 mJm^{-2}, in close agreement with the DFT calculations mentioned above. However, the comparison must be viewed cautiously, as the DFT calculations do not include van der Waals interactions. The fact that the work of adhesion, as a result of all other nonspecific electronic interactions predicted by the DFT calculations (8 mJm^{-2}), does not exceed the measured value (10.4 ± 4) demonstrates reassuring consistency. Note the dramatic reduction of adhesion as compared with the Si–Si interface.

Bulk chemistry

The mechanical and tribological properties of DLC films are strongly affected by their bulk chemistry, most notably, the H content and the sp^2/sp^3 bonding ratio[28,61,62]. However, these two parameters are difficult to study separately because it is difficult to grow films that vary one of these independently of the other.

Some initial studies have been attempted using diamond AFM tips. Jiang *et al.*[62] have measured nanohardness, wear, and friction on thin, magnetron-sputtered DLC films. Using H concentrations of ~2 at. %, 28 at. %, and 40 at. %, they have found that the friction coefficient increases and hardness and wear performance decreases with higher H concentration. Unfortunately, the sp^3/sp^2 bonding ratios in the films have not been specified. In a related macroscale study, macroscopic friction coefficients for DLC films grown in a very similar fashion are lowest when the films were grown with ~25% H content[57], suggesting that an optimal H concentration may exist. In fact, the lowest friction and wear for NFC films occurs at an optimal intermediate H concentration[8], and so further study of this effect is desirable.

DLC films grown using microwave plasma chemical vapor deposition (MPCVD) technique have been tested as a function of H_2 (g) in the plasma[63]. Increasing the plasma's H_2 (g) concentration leads to a higher sp^3 bonding fraction, lower friction, and improved wear performance, as measured by AFM with a diamond tip. Unfortunately, neither the percentage of H in the film nor the sp^2/sp^3 bonding ratio were quantified, and so the effects observed cannot be definitively linked to film structure.

While it is clear that the amount of H and the sp^3/sp^2 bonding ratio influence nanotribology, detailed comprehensive studies necessarily involve varying these parameters independently to elucidate their individual contributions to the mechanical and tribological behavior.

In an attempt to investigate the influence of sp^2/sp^3 bonding ratio in amorphous carbon (a-C) directly, DLC films with either 34% or 53% sp^3 bonding were deposited in a pulsed laser deposition (PLD) system[28]. The hardness and elastic modulus increases with increasing sp^3 content as expected, but in this case friction, when sliding a Si_3N_4 tip across each surface, is unaffected. CN_x films have been grown with various N content ($0.2 < x < 0.3$, corresponding to 36–53% sp^3 bonding), and again the resistance to sliding does not depend on the

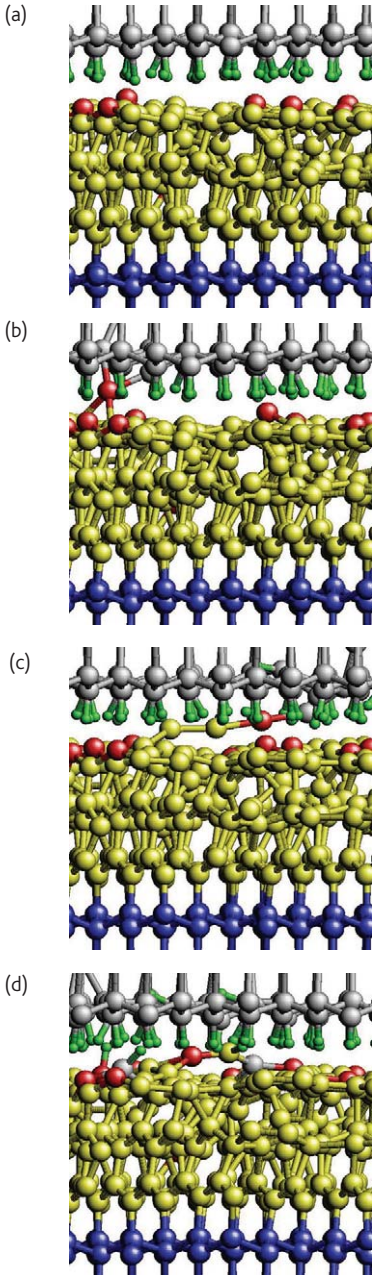

Fig. 9. A series of tribochemical reactions that occur when a H-terminated diamond counterface slides against a H-free a-C film. The load is 230 nN. From top to bottom: the counterface has slid 0.0 nm, 1.35 nm, 2.35 nm, and 14.45 nm. Prior to sliding (a), several unsaturated sp-hybridized C atoms (red) are present on the surface of the film. A chemical bond is formed between the diamond counterface (gray) and the sp-hybridized atom (b). Both the counterface and the film undergo significant restructuring as a result of the adhesive bond formation (c). In (c), a number of atoms are being 'pulled' from the film. Continued sliding causes adhesive bonds to rupture, leading to the transfer of counterface atoms to the film and significant restructuring of the film (d). Counterface C and H atoms are shown in gray and green, respectively. Unsaturated sp-hybridized atoms in the film are shown in red and the remaining film atoms are shown in yellow. Diamond substrate atoms are shown in blue. (Reproduced with permission from[64]. © 2003 American Chemical Society.)

sp^2/sp^3 bonding ratio. Overall, the DLC films exhibit higher nanoscale friction than the CN_x films, and both films exhibit significantly higher friction than HOPG (by an order of magnitude).

Gao *et al.*[64], who have also studied the in variations in the sp^2/sp^3 ratio of DLC, have carried out MD simulations showing that this ratio alone does not determine the mechanical properties of the films; rather, the three-dimensional structure of these bonds must be considered. For example, films with sp^2-hybridized rings oriented perpendicular to the substrate can have larger elastic constants than films with a higher sp^3 bonding percentage. When two surfaces composed of sp-, sp^2- and sp^3-hybridized bonds slide against one another, the sp-bonded carbon atoms are observed to be the most reactive components responsible for tribochemistry and wear (Fig. 9). This work provides evidence that tribochemical reactions occurring within the bulk of a film, as well as across a sliding interface, play a role in determining tribological performance.

The incorporation of F has been found to alter the hydrophobicity of DLC films, and this affects the frictional characteristics as well[65]. Using a CVD process, increasing the F concentration increases the water contact angle (from 72–95°, as F content is increased from 0–35 at. %). Correspondingly, adhesion and friction measured by AFM in air decreases with increasing contact angle. The reduced adhesion may be the result of the reduction of capillary interactions, but the presence of a capillary has not been observed directly. Regardless, this demonstrates the important influence that adhesion forces have on nanoscale friction.

New perspectives gained from these investigations indicate that for hard carbon systems, surface chemistry dominates the tribology in the wearless regime, while bulk chemistry matters more after the wear threshold has been crossed.

Influence of environment

The humidity dependence of the macrotribological properties of DLC and diamond has been well-documented[16]. Tribochemical reactions do occur, but physisorption of environmental species also plays a role. An understanding of how humidity affects these materials nanoscopically is only beginning to emerge. For example, for a Si_3N_4 AFM tip on a DLC film grown by a plasma source ion deposition process, friction in the wearless regime exhibits a monotonic and reversible change when the relative humidity (RH) is increased from <5% to 60%, increasing with higher humidity[66]. This corresponds to a ~40% increase in interfacial shear strength. Surprisingly, the adhesion shows no dependence on RH. These results indicate that the conventional picture of meniscus formation leading to higher friction and adhesion does not represent the mechanism at play in this system, since the adhesion should change with RH. The authors propose that physisorbed water apparently increases the shear strength.

Using hydrocarbon-coated AFM tips, Schwarz *et al.*[39] have found that the frictional properties of diamond and amorphous carbon differ between air (at 40–60% RH) and dry Ar environments. Interfacial shear strengths are found to be highest for a-C in air, followed by diamond in air, then a-C in dry Ar, and finally diamond in dry Ar. Adhesive forces are also lower in the dry Ar environment. They attribute the higher friction in ambient conditions to the presence of water on the surface of the samples. They also suggest that surface contamination from the environment could play a significant role. Both of these studies are qualitatively consistent with the MD models of Gang *et al.*[67], who have found that the adsorption of third bodies (such as hydrocarbon contamination) onto clean surfaces of incommensurate crystalline or amorphous materials can increase static friction. The trapped molecules arrange themselves in sites that increase interfacial friction, which would otherwise be extremely low for these incommensurate surfaces.

Other adsorbed species have also been considered. MD simulations with methane molecules in between two H-terminated diamond surfaces show that friction is reduced compared with sliding in their absence[68,69]. The lattice vibrations excited at the diamond surfaces determine the friction-load dependence. Without methane, increasing the load increases the amount of vibrational excitation of the lattice and therefore the friction. When methane is trapped between the surfaces, the vibrational excitation initiated in the upper diamond lattice by the sliding is very small, resulting in a lower resistance to sliding.

Influence of substrate material, thickness, and roughness

Other important factors are film thickness, substrate roughness, and substrate stiffness[70–74]. For hard carbon coatings on substrates, of particular interest for hard-disk applications, numerous groups have reported that a critical film thickness (usually >5 nm) needs to be achieved for the coating to exhibit the exceptional nanoscale friction and wear properties known to these materials[71,74]. Additionally, the roughness and modulus of the substrate can affect coating properties. As a result, the conformal way in which ta-C and DLC films coat a substrate, substrate roughness is transferred to the coating. A lower elastic modulus of the substrate can lead to bending under applied loads, which can lead to increased contact area and thus friction[70]. As coating thickness reaches a practical lower limit, determining the intrinsic properties and likewise the functionality of the coatings for wear- and corrosion-resistant applications poses a challenge.

Carbon nanotips

Standard commercial AFM cantilevers with integrated tips (typically Si or Si_3N_4) often get damaged when the tip snaps into contact or when they slide across an abrasive surface at increased loads[75–78]. They can also become easily contaminated[79,80]. The use of hard carbon materials, such as diamond, for AFM tips can produce sharp, wear-resistant, stable, and inert surface probes for nanoscale

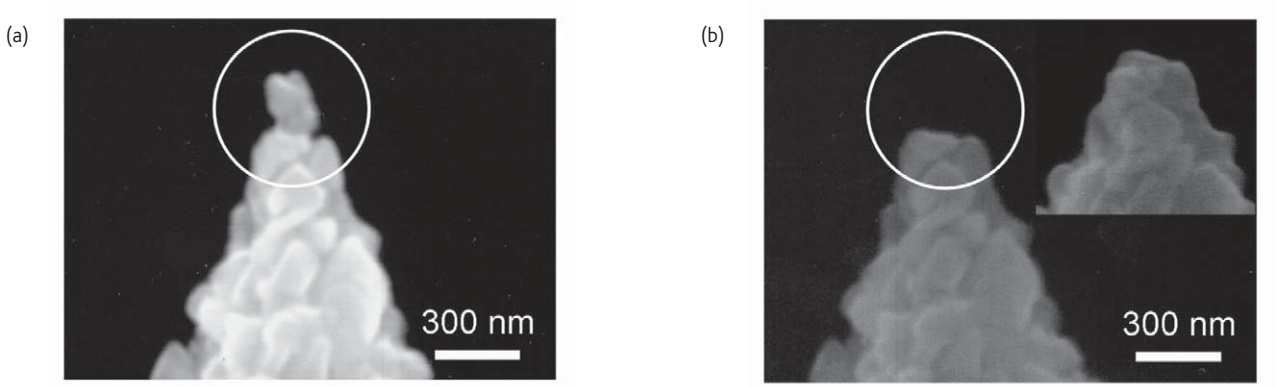

Fig. 10 Scanning electron micrographs of a diamond-coated probe (a) before and (b) after a 450 mm sliding distance on a Cu specimen with an inset of the tilted view. (Reproduced with permission from[88]. © 2007 Elsevier.)

tribological and electrical investigations. For over a decade, various research groups have been fabricating these diamond and hard carbon AFM tips[39,44,81–87]. Efforts to fabricate diamond tips have involved several methods, namely: growing diamond polycrystallites on the apexes of standard AFM cantilever tips to reduce mechanical degradation[44,83,88], focused ion beam (FIB) milling of B-doped diamond AFM tips for electrical characterization[89], and batch fabricating diamond CVD diamond tips using molding techniques to reproducibly make high aspect ratio, sharp (radius of curvature <20 nm) tips for high-resolution imaging[81,85–87]. When quantitatively evaluated, the wear performance of crystalline diamond-coated tips is shown to involve initial removal of a-C present at the surface, and subsequently results in gradual wear of the tip on a Si_3N_4 surface[88] (Fig. 10). Failure to form a continuous diamond coating on the tip (as diamond films are challenging to nucleate on Si), and/or subsequent delamination of the film during use, are difficult challenges. Other researchers[39,42] have produced hard a-C coatings on tips (Fig. 11), and the robustness of these coatings has been demonstrated by scanning single-crystal diamond surfaces at appreciable contact stresses and seeing no observable changes in the transmission electron microscope (TEM)[39,42]. Thus, if the film is continuous and well adhered, performance is excellent. This indicates that carbon-based tips are highly promising not only to enable the study of carbon nanotribology more reliably, but to enable a whole range of more sophisticated, reliable, and demanding scanning probe microscopy applications.

Summary and future

The fascinating interdisciplinary science of nanotribology brings together tools and ideas from physics, mechanics, materials science, chemistry, and beyond. There is still much to be learned by experimenting with and simulating tribological interaction of these diverse carbon-based materials. Connecting nanoscale and micro/macroscale friction behavior remains a challenge. The length and time scales of nanotribology experiments and molecular simulations are still separated by orders of magnitude. Better control and characterization of the AFM tip is needed, and is indeed starting to emerge in the latest studies.

Sophisticated experimental techniques and advanced computational techniques continue to reveal unexpected and exciting behavior, and the importance of characterizing the detailed material structure and environmental conditions is becoming increasingly clear. As the technology of specialized carbon materials advances, our understanding of the physical origins of friction, adhesion, energy dissipation, and wear at the atomic-scale must continue to evolve.

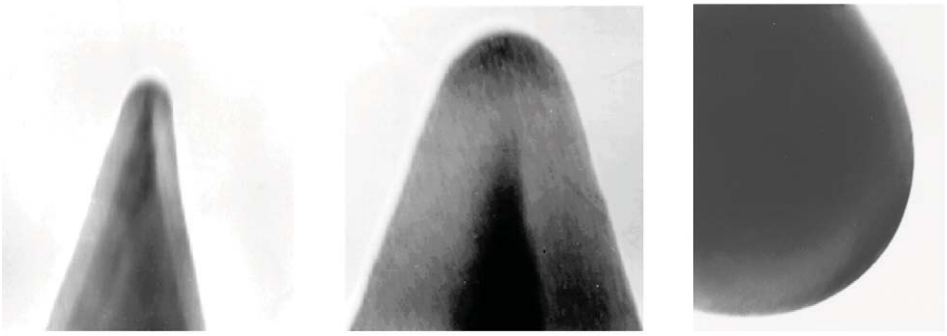

Fig. 11 Transmission electron micrographs of three different tips with spherical apexes prepared using electron beam induced decomposition inside the TEM. (Reproduced with permission from[39]. © 1997 American Physical Society.)

REFERENCES

1. Novoselov, K. S., *et al.*, *Science* (2004) **306**, 666
2. Dahl, J. E., *et al.*, *Science* (2003) **299**, 96
3. Robertson, J., *Amorphous Carbon: State of the Art*. Silva, S. R. P., *et al.* (eds.), World Scientific, Cambridge, (1998), 361
4. Robertson, J., *Mater. Sci. Eng. R.* (2002) **37**, 129
5. Auciello, O., *et al.*, *Proc. SPIE-Int. Soc. Opt. Eng.* (2001) **4235**, 10
6. Philip, J., *et al.*, *J. Appl. Phys.* (2003) **93**, 2164
7. Erdemir, A., *et al.*, *Surf. Coat. Technol.*, (1999), **120–121**, 565
8. Erdemir, A., and Donnet, C., *Modern Tribology Handbook*. Bhushan, B., (ed.), CRC Press, Boca Raton, (2001) **2**, 465
9. Auciello, O., *et al.*, *J. Phys.: Condens. Matter* (2004) **16**, R539
10. Sullivan, J. P., *et al.*, *Mat. Res. Soc. Symp. Proc.* (2001) **657**, EE711
11. Kohn, E., *et al.*, *New. Diamond Front. Carbon Technol.* (2001) **11**, 81
12. Andersson, J., *et al.*, *Surf. Coat. Technol.* (2003) **163–164**, 535
13. Dickrell, P. L., *et al.*, *J. Tribol.* (2005) **127**, 82
14. Heimberg, J. A., *et al.*, *Appl. Phys. Lett.* (2001) **78**, 2449
15. Gao, F., *et al.*, *Tribol. Lett.* (2005) **20**, 221
16. Kim, H. I., *et al.*, *Tribol. Lett.* (2006) **21**, 51
17. Gardos, M. N., and Soriano, B. L., *J. Mater. Res.* (1990) **5**, 2599
18. Gardos, M. N., and Gabelich, S. A., *Tribol. Lett.* (1999) **6**, 87
19. Gardos, M. N., and Gabelich, S. A., *Tribol. Lett.* (1999) **6**, 103
20. van den Oetelaar, R., and Flipse, C., *Surf. Sci.* (1997) **384**, L828
21. Maboudian, R., *et al.*, *Tribol. Lett.* (2002) **12**, 95
22. Carpick, R. W., and Salmeron, M., *Chem. Rev.* (1997) **97**, 1163
23. Carpick, R. W., *et al.*, *J. Vac. Sci. Technol., B* (1996) **14**, 1289
24. Carpick, R. W., *et al.*, *Langmuir* (1996) **12**, 3334
25. Carpick, R. W., *et al.*, *Appl. Phys. Lett.* (1997) **70**, 1548
26. Carpick, R. W., *et al.*, *Fracture and Ductile vs. Brittle Behavior – Theory, Modeling and Experiment.*, Beltz, G., *et al.* (eds.), Materials Research Society, Warrendale, (1999), 93
27. Enachescu, M., *et al.*, *Tribol. Lett.* (1999) **7**, 73
28. Riedo, E., *et al.*, *Surf. Sci.* (2001) **477**, 25
29. Hertz, H., *J. Reine Angew. Math.* (1881) **92**, 156
30. Johnson, K. L., *Proc. R. Soc. London, Ser. A* (1997) **453**, 163
31. Israelachvili, J. N., *Intermolecular and Surface Forces*, Academic Press, London, (1992)
32. Johnson, K. L., *et al.*, *Proc. R. Soc. London, Ser. A* (1971) **324**, 301
33. Derjaguin, B. V., *et al.*, *J. Colloid Interface Sci.* (1975) **53**, 314
34. Johnson, K. L., *Contact Mechanics*, Cambridge University Press, Cambridge, (1987)
35. Unertl, W. N., *J. Vac. Sci. Technol., A* (1999) **17**, 1779
36. Luan, B., and Robbins, M. O., *Nature* (2005) **435**, 929
37. Luan, B., and Robbins, M. O., *Phys. Rev. E: Stat. Phys., Plasmas, Fluids, Relat. Interdiscip. Top.* (2006) **74**, 26111
38. Buzio, R., *et al.*, *Wear* (2003) **254**, 981
39. Schwarz, U. D., *et al.*, *Phys. Rev. B: Condens. Matter* (1997) **56**, 6987
40. Carpick, R. W., *et al.*, *J. Occup. Med.* (2004) **56**, 48
41. Enachescu, M., *et al.*, *Phys. Rev. Lett.* (1998) **81**, 1877
42. Gao, G., *et al.*, *Langmuir* (2007) **23**, 5394
43. Enomoto, Y., and Tabor, D., *Proc. R. Soc. London. A* (1981) **373**, 405
44. Germann, G. J., *et al.*, *J. Appl. Phys.* (1993) **73**, 163
45. Harrison, J. A., *et al.*, *Wear* (1993) **168**, 127
46. Mate, C. M., *et al.*, *Phys. Rev. Lett.* (1987) **59**, 1942
47. Medyanik, S. N., *et al.*, *Phys. Rev. Lett.* (2006) **97**, 136106
48. Johnson, K. L., and Woodhouse, J., *Tribol. Lett.* (1998) **5**, 155
49. Socoliuc, A., *et al.*, *Phys. Rev. Lett.* (2004) **92**, 134301
50. Krylov, S. Y., *et al.*, *Phys. Rev. Lett.* (2006) **97**, 166103
51. Dienwiebel, M., *et al.*, *Phys. Rev. Lett.* (2004) **92**, 126101
52. Dienwiebel, M., *et al.*, *Surf. Sci.* (2005) **576**, 197
53. Kis, A., *et al.*, *Phys. Rev. Lett.* (2006) **97**, 025501
54. Grillo, S. E., and Field, J. E., *Wear* (2003) **254**, 945
55. Grillo, S. E., and Field, J. E., *J. Phys. D: Appl Phys* (2000) **33**, 595
56. Gao, G. T., *et al.*, *J. Am. Chem. Soc.* (2002) **124**, 7202
57. Zhang, S., *et al.*, *Surf. Coat. Technol.* (2004) **177–178**, 818
58. Qi, Y., *et al.*, *Surf. Sci.* (2006) **600**, 2955
59. Sumant, A. V., *et al.*, *Adv. Mater.* (2005) **17**, 1039
60. Sumant, A. V., *et al.*, unpublished results
61. Glosli, J. N., *et al.*, *J. Comput.-Aided Mater. Des.* (1996) **3**, 233
62. Jiang, Z., *et al.*, *Thin Solid Films* (1995) **258**, 75
63. Fang, T. H., *et al.*, *Thin Solid Films* (2001) **396**, 167
64. Gao, G. T., *et al.*, *J. Phys. Chem. B* (2003) **107**, 11082
65. Prioli, R., *et al.*, *Tribol. Lett.* (2003) **15**, 177
66. Flater, E. E., *et al.*, *Polym. Mater. Sci. Eng.* (2004) **90**, 197
67. Gang, H., *et al.*, *Science* (1999) **284**, 1650
68. Perry, M. D., and Harrison, J. A., *J. Phys. Chem. B* (1997) **101**, 1364
69. Perry, M. D., and Harrison, J. A., *Thin Solid Films* (1996) **291**, 211
70. Staedler, T., and Schiffmann, K., *Surf. Sci.* (2001) **482-485**, 1125
71. Sundararajan, S., and Bhushan, B., *Wear* (1999) **225-229**, 678
72. Lu, W., and Komvopoulos, K., *J. Tribol.* (2001) **123**, 717
73. Beake, B. D., and Lau, S. P., *Diamond Relat. Mater.* (2005) **14**, 1535
74. Zhaoguo, J., *et al.*, *IEEE Trans. Magn.* (1995) **31**, 3015
75. Liu, H., *et al.*, *J. Vac. Sci. Technol., B* (2005), **23**, 3090
76. Larsen, T., *et al.*, *Appl. Phys. Lett.* (2002) **80**, 1996
77. Kopycinska-Mueller, M., *et al.*, *Mater. Res. Soc. Symp. Proc.* (2006) **924**, 19
78. Chung, K.-H., *et al.*, *Ultramicroscopy* (2005) **102**, 161
79. Qian, L. M., *et al.*, *Langmuir* (2000) **16**, 662
80. Brukman, M. J., *et al.*, *Langmuir* (2006) **22**, 3988
81. Beuret, C., *et al.*, *Appl. Phys. Lett.* (2000) **76**, 1621
82. Shibata, T., *et al.*, *Transducers, Solid-State Sensors, Actuators and Microsystems Tech. Digest* (2003) **1**, 500
83. Tanasa, G., *et al.*, *J. Appl. Phys.* (2003) **94**, 1699
84. Olbrich, A., *et al.*, *J. Vac. Sci. Technol., B* (1999), **17**, 1570
85. Hantschel, T., *et al.*, *Microelectron. Eng.* (2001) **57–58**, 749
86. Shibata, T., *New Diamond Front. Carbon Technol.* (2000) **10**, 161
87. Kim, K. H., *et al.*, *Small* (2005) **1**, 866
88. Chung, K.-H., and Kim, D.-E., *Ultramicroscopy,* (2007) in press
89. Olbrich, A., *et al.*, *J. Vac. Sci. Technol., B* (1999) **17, 1570**